

# Differential Scanning Calorimetry of Plasma Proteome: Identifying Diagnostic Signatures in Alzheimer's Disease

Tobías Ledesma<sup>1</sup>, Lorenzo Campanelli<sup>2</sup>, Micaela Bulacio<sup>1</sup>, Patricia Solis<sup>3</sup>,  
María C. Dalmasso<sup>3</sup>, Laura Morelli<sup>2~</sup> and Mariano Dellarole<sup>1~</sup>

<sup>1</sup>CIBION-CONICET, Godoy Cruz 2390, Buenos Aires, Argentina.

<sup>2</sup>Laboratory of Brain Aging and Neurodegeneration, Fundación Instituto Leloir, IIBBA-CONICET. Av. Patricias Argentinas 435. Ciudad Autónoma de Buenos Aires, Argentina.

<sup>3</sup>Studies in Neuroscience and Complex Systems Unit (CONICET-HEC-UNAJ). Av. Calchaquí 5402, Florencio Varela, Argentina.

<sup>~</sup>Correspondence should be addressed to [LMorelli@leloir.org.ar](mailto:LMorelli@leloir.org.ar) & [mdellarole@cibion.gov.ar](mailto:mdellarole@cibion.gov.ar).

## Abstract

Differential scanning calorimetry (DSC) offers an innovative method for evaluating serum proteome profiles as a diagnostic tool. In this study, we examined serum samples from 13 patients diagnosed with Alzheimer's disease (AD) and 12 healthy elderly (HE) individuals, to explore DSC's potential in identifying biochemical alterations associated with AD. Each thermogram was generated by gradually heating the samples from 35°C to 100°C at a rate of 1°C per minute, using 20 µL of serum diluted 35-fold in PBS. The thermograms of healthy individuals exhibited a consistent, characteristic profile, while those of AD patients displayed distinct deviations. Notably, the thermal scans of AD samples revealed a significant displacement of 1.3°C in the albumin peak compared to healthy samples and the emergence of a novel peak at 53.4°C. These variations suggest possible modifications in albumin structure due to interactions with disease-specific biomarkers or post-translational modifications. Our findings underscore DSC's utility as a non-invasive, cost-effective diagnostic tool for early detection and monitoring of AD, facilitating timely clinical interventions and promoting healthier aging.

**Keywords:** Differential scanning calorimetry, Serum proteome, Alzheimer's disease, Thermogram analysis, thermal liquid biopsy.

## Introduction

Differential Scanning Calorimetry (DSC) is a technology that enables the direct measurement of thermal stability of biomolecules in solution by recording the specific heat capacity as a function of temperature. In multicomponent systems, such as biological fluids, the DSC profile describes the thermal stability summation of the individual contributions plus variations owing to interactions among them<sup>1</sup>. Recently, Dr. Garbett and collaborators revealed that the DSC profile of human plasma or serum shows the cumulative contributions of the most abundant protein components, mainly albumin, immunoglobulins IgA, IgG and IgM, transferrin, haptoglobin, complement C3 and in plasmatic samples fibrinogen<sup>2</sup>, thereby representing a global thermal stability sensible to their proportion, interaction and posttranslational modification state<sup>3</sup>. Notably, the DSC thermograms of serum or plasma from healthy individuals show a robust profile regardless of ethnicity, sex, age, and habits but significant deviations in sick patients<sup>4</sup>. DSC presented sensitivity to several cancers<sup>3,5,6,7,8,9,10,11</sup>, and also to autoimmune diseases<sup>4,12</sup>, endocrine and metabolic Diseases<sup>13</sup>, infectious diseases<sup>4</sup>, cardiovascular and pulmonary diseases<sup>14,15</sup> and pregnancy-related conditions<sup>8</sup>.

The sensitivity of this technique to changes in plasmatic homeostasis was also addressed to neurological diseases, for instance Parkinson, Amyotrophic lateral sclerosis and Schizophrenia<sup>16,17</sup> but, to our knowledge, not for Alzheimer's disease (AD). Brain imaging techniques, PET and MRI, remain fundamental in the diagnosis of AD. These allow the visualization of beta-amyloid plaques, brain atrophy, and other structural changes, providing valuable information in the diagnostic process. Although biomarker analysis in cerebrospinal fluid (CSF) has advanced in the detection of tau protein and beta-amyloid peptide, the invasiveness of this technique limits its widespread clinical application, and research is being carried out with a high emphasis on detection techniques for AD and dementia in blood. Novel evidence shows the presence or alterations of plasmatic proteome as prominent AD biomarkers<sup>18</sup>, including the accumulation of posttranslational modification of albumin via deamidation<sup>19,20,21</sup>. This data suggests that AD patients' may also present characteristic DSC signatures on their plasma.

By 2050, the aging population will significantly increase the prevalence of dementia, particularly Alzheimer's disease (AD), which is already a leading cause of mortality and morbidity. Enhancing the early detection of AD is key, not only because it is a progressive neurodegenerative disease of gradual deterioration of cognitive functions, but because of the novel monoclonal early-stage AD therapies targeting amyloid- $\beta$  (A $\beta$ ) aggregates<sup>22,23,24</sup>. This research explores serum samples from healthy elderly individuals and AD patients using DSC in order to identify distinct attributes among

these groups. We introduce a novel method to standardize the thermogram analysis based on Gaussian curves. We show that AD thermograms present a characteristic peak shift and also the presence of an additional peak in comparison with healthy elderly individuals. Our study reinforces the use of this centenary technology to address neurological disorders in a timely manner.

v1 Preprint

## Results

**Calorimetric profile of plasma from healthy elderly individuals.** Plasma from healthy elderly (HE) volunteers (75 to 85 years old) was analyzed by DSC in order to understand and define an average thermogram for HE to use as a reference for dementia (Fig. 1). HE volunteers are a sensible cohort because of symptomless age related diseases. Because of the capacity of the technique to address common complications<sup>14</sup> we have selected a pool of 12 HE discarding profiles to avoid undiagnosed diseases, sample handling issues (data not shown). The HE volunteers profile shows an average in excellent agreement with data measured previously by other laboratories for standard healthy individuals<sup>4,25,26</sup>. Our data expands the robustness of the approach in monitoring the healthiness of elderly.

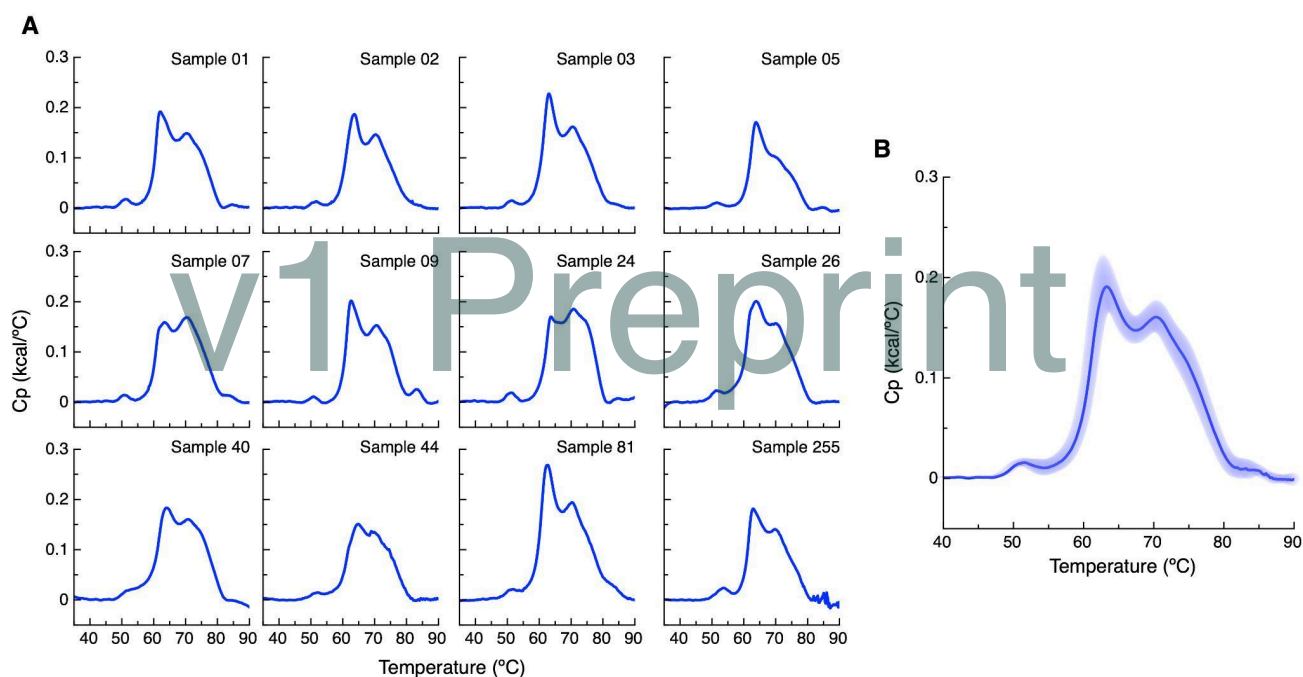


Figure 1: Healthy Elderly Thermograms. (A) DSC profiles of twelve healthy elderly volunteers plasma. (B) DSC average profile of Healthy Elderly cohort with the corresponding standard deviation shown in light blue.

**Alzheimer's Disease Thermograms.** We have analyzed plasma samples of a cohort of 13 patients diagnosed with Alzheimer's disease by DSC (Fig. 2). Each profile was subtracted to the HE average profile in order to address significant changes. The AD thermograms presented slight changes with respect to the HE average profile, with variations below 0.1 kcal/°C. However, in most of the cases we can appreciate a common differential pattern with a “heartbeat sinus rhythm” like shape. The consistency of the pattern becomes evident on the averaged data profiles (Fig. 2 B). The differences

on AD profiles appear to denote a shift to higher temperature of the main plasma peak located between 60 and 65°C. This peak is attributed to the thermal denaturation of the albumin protein, corresponding to around 60% in mass (a concentration of around 45 mg/ml)<sup>27</sup> of the plasma proteome. This albumin shift plus differences shown below the albumin peak, at temperatures corresponding to the first peak, located between 50 and 55°C of HE profiles (Fig. 2B), lead the observed *heartbeat* differential pattern. The first peak was related to Fibrinogen, a protein representing around 3% of the total proteome (a concentration of around 3 mg/ml)<sup>27</sup>, and shown to be a protein absent in serum samples and inert to interactions or changes on DSC disease profiles<sup>2</sup>. Overall, the average deviations among HE and AD profiles showed slight but significant differences that were explored as AD signatures.

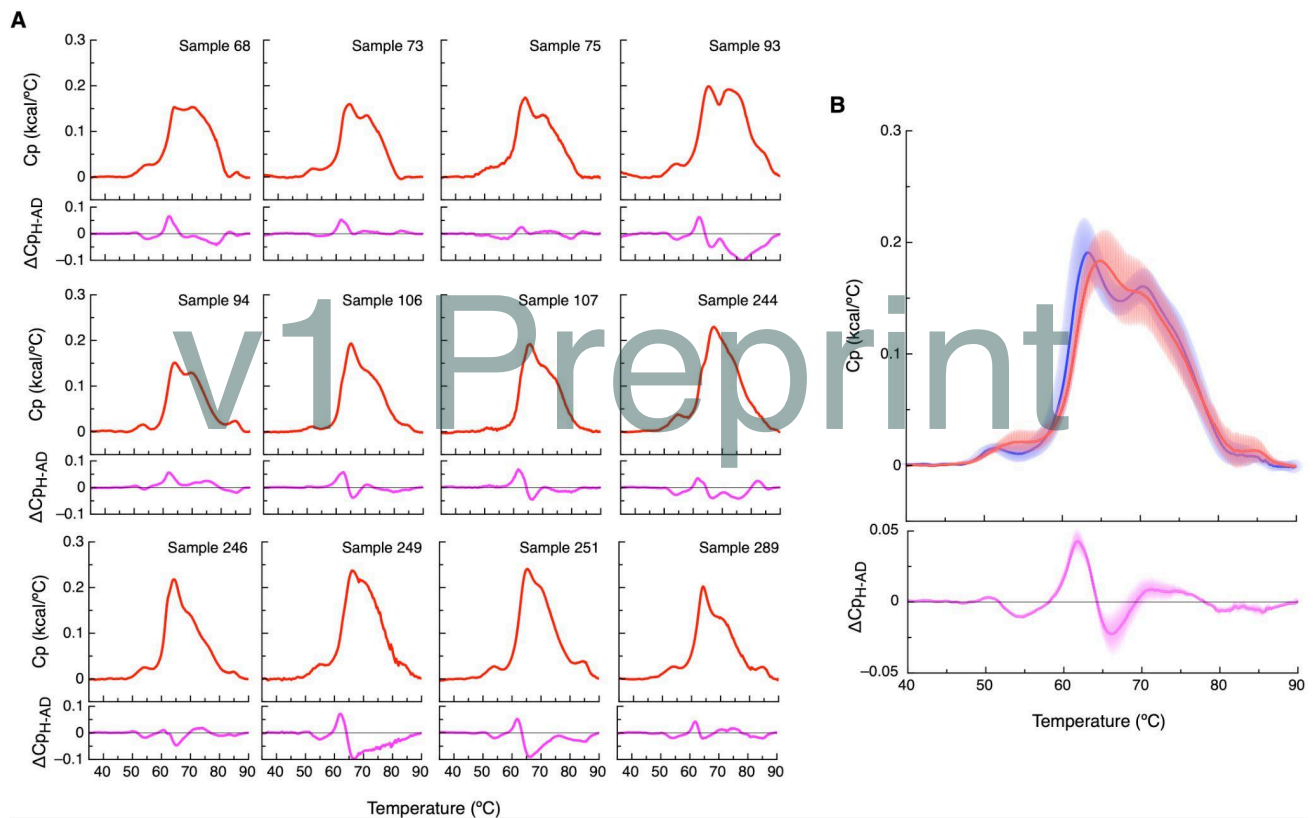


Figure 2: AD patients Thermograms. (A) Thermogram of twelve AD patients (red lines) and the corresponding differential profile against the healthy elderly average (pink lines, lower panels). (B) Top panel, DSC profile of Healthy Elderly (blue line) and AD patients (red line) averages with the corresponding standard deviation in light blue. Bottom panel, DSC differential profile between Healthy Elderly and AD patients averages.

**Alzheimer's DSC signatures.** Because the DSC of plasma is not thermally reversible, their interpretation is hypothesis and model free. Several works have presented different numerical approaches for the parametrization of DSC profiles<sup>8,28,29</sup> but, to date there is no consensus and each

methodology was adapted to the disease using the local knowledge. In order to address the observed differences we developed a simple method accordingly. The global sum of Gaussian Peaks bona fide denote the thermograms:

$$A \cdot \exp\left(\frac{-(x-x_0)^2}{2s^2}\right), \text{ of } A \text{ amplitude; } x \text{ maximum peak value and } s \text{ the width at half of the peak.}$$

While HE demanded 5 Gaussian Peaks, in all but 3 of the AD DSC profiles an additional peak between the fibrinogen and albumin peaks was needed for a bonafide fitting, see Fig 3A and B. While the average HE and AD fibrinogen peak has a maximum of  $51.2 \pm 0.3$  °C, in agreement with the literature<sup>4</sup>, the AD novel peak has a maximum of  $53.4 \pm 0.2$  °C (Table 1).

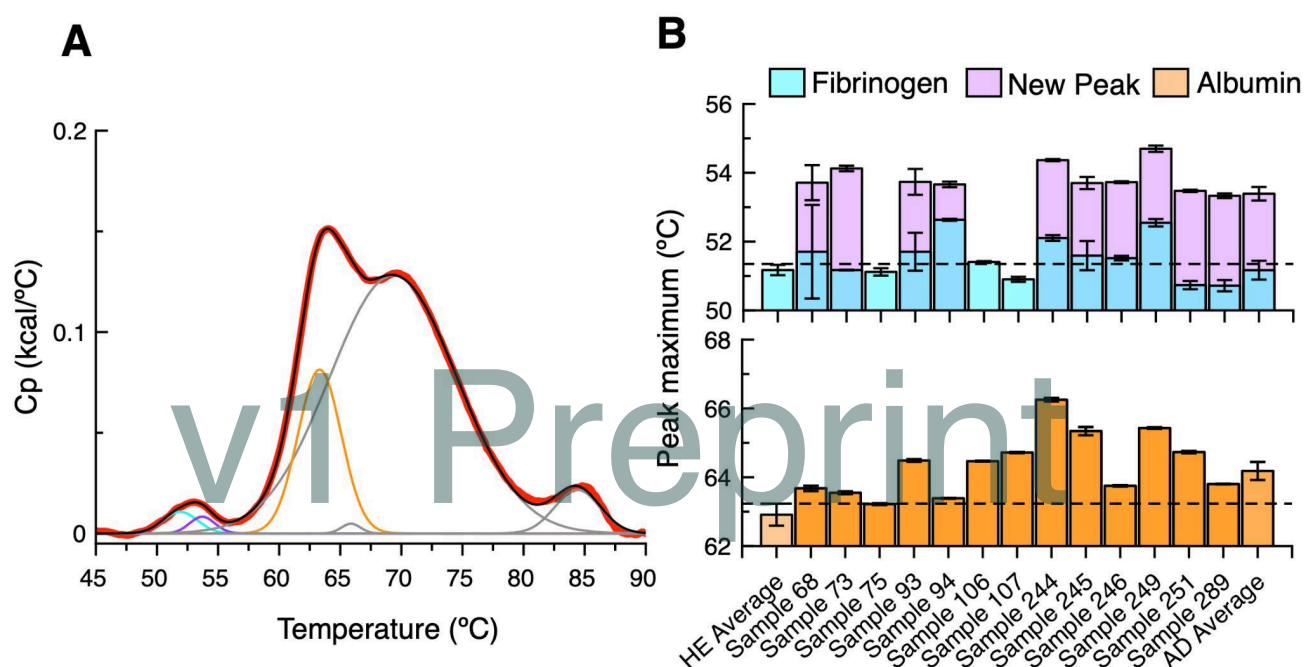


Figure 3: Parametrization of thermograms. A) Data fitting to gaussian peaks. Example of sample 94 data (red line) fitting (black dotted line) to six gaussian peaks, colored cyan for the so-called fibrinogen peak, violet for the so-called new peak, orange for the so-called albumin peak and the others peaks in gray. B) Histogram of peak maximum temperature for the albumin, fibrinogen and the new peak colores as in panel A. The peak values of the healthy elderly (HE) and AD patients asr also shown. Dashed lines show the HE average plus two SDEV values.

In order to complete the observed heartbeat signature, we focused on the albumin peak. All DSC AD profiles presented a higher thermal albumin peak maxima, with an average shift of  $1.3 \pm 0.3$  °C (Fig 3 and Table 1). It has recently been documented an association between the presence of deamidated albumin and AD. The hypothesis is supported by evidence showing that deamidated albumin is incapable of binding amyloid beta peptides (A $\beta$ ) and phosphorylated tau (p-tau) proteins, leading to progressive accumulation of them in the brain<sup>19</sup>. Deamidation in albumin is an aging process that

leads to the formation of isoaspartate (isoAsp) on different asparagine residues and its clearance can be affected due to age-related liver fails<sup>20</sup>. We have measured the DSC profile of pure Human Serum Albumin (HSA) and deamidated induced albumin in order to understand the effect of the observed DSC AD attributes. Interestingly, the heat induced protocol to deamidate the HSA albumin shows a highest melting temperature, (Table 1), indicating that the AD shift for the albumin main peak profile could be influenced by aging related post translational modifications.

**Table 1.** Thermogram parametrization.

Samples	Albumin main Peak	Fibrinogen Peak	New Peak
	T <sub>m</sub> (°C)	T <sub>m</sub> (°C)	T <sub>m</sub> (°C)
Healthy Average	62.91 ± 0.32	51.17 ± 0.01	Undetected
Sample 68	63.68 ± 0.08	51.71 ± 1.36	53.71 ± 0.51
Sample 73	63.55 ± 0.04	51.17 ± 0.01	54.13 ± 0.08
Sample 75	63.22 ± 0.03	51.12 ± 0.11	Undetected
Sample 93	64.49 ± 0.04	51.70 ± 0.55	53.74 ± 0.38
Sample 94	63.39 ± 0.01	52.63 ± 0.03	53.66 ± 0.08
Sample 106	64.47 ± 0.01	51.41 ± 0.03	Undetected
Sample 107	64.72 ± 0.02	50.90 ± 0.07	Undetected
Sample 244	66.25 ± 0.05	52.10 ± 0.08	54.37 ± 0.03
Sample 245	65.34 ± 0.12	51.59 ± 0.42	53.70 ± 0.18
Sample 246	63.75 ± 0.02	51.52 ± 0.07	53.73 ± 0.03
Sample 249	65.43 ± 0.02	52.55 ± 0.11	54.70 ± 0.09
Sample 251	64.73 ± 0.03	50.74 ± 0.12	53.47 ± 0.03
Sample 289	63.80 ± 0.01	50.72 ± 0.16	53.33 ± 0.07
AD Average	64.18 ± 0.26	51.17 ± 0.27	53.39 ± 0.20
Pure HSA	61.2 ± 0.1	—	—
Deamidated HSA	83.3 ± 0.1	—	—



## Discussion

The rising prevalence of AD is a global emergency, according to Alzheimer's Association<sup>30</sup>, an estimated 6.9 million Americans age 65 and older are living with AD in 2024. Seventy-three percent are 75 or older and about 1 in 9 people aged 65 and older (10.9%) has Alzheimer's. Effective and minimally invasive approaches of AD's diagnosis is a priority. Upon comparison against HE DSC scans, we show that the DSC thermograms of AD patients' plasma displays signatures for its introduction as a diagnostic guide and general monitoring of healthiness over elderly individuals. The simplicity of the technique can be imagined in a simple monitoring scheme adapted to a preventive healthcare system (Fig. 4).

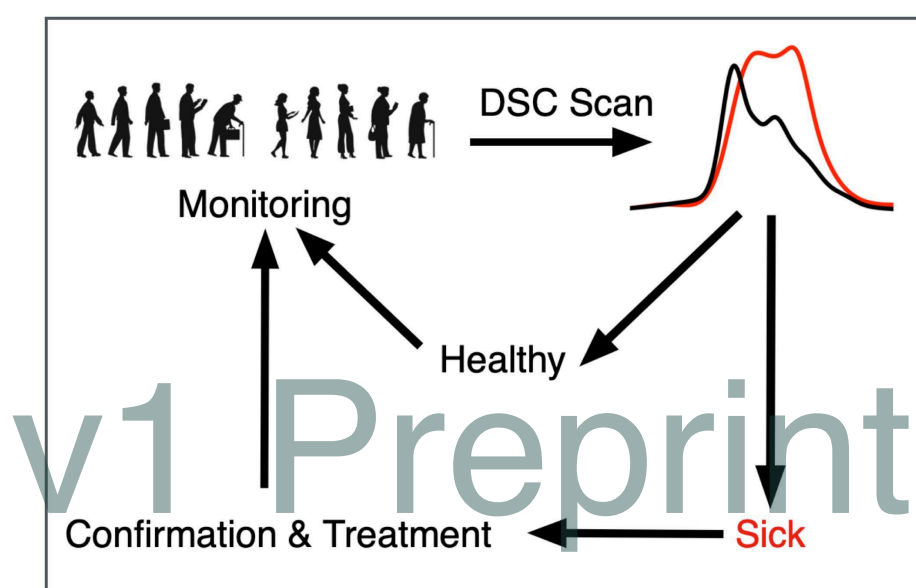


Figure 4. Monitoring Scheme for Neurological Disorders. The flow we foresee for the implementation of DSC as guide for healthy aging comprehends a recurrent monitoring of patients prior and during the disease treatment as a complementary healthcare support system.

We evaluated the plasma proteome of AD and long-lived healthy patients in search of potential markers that could distinguish the studied pathology from the healthy state. Protein aging events, such as isoaspartate formation, were associated with alterations in protein structure and function with an impact on age-related diseases<sup>21</sup>. It was suggested that in the case of AD, the formation of isoaspartate in albumin, HSA, leads to a reduction in its ability to transport ligands, such as A $\beta$  and p-tau. This reduction favors the aggregation of A $\beta$  and p-tau in the brain, thus increasing the risk of Alzheimer's disease<sup>20</sup>. Isoaspartate, as a result of spontaneous deamidation, damages protein structures, making them prone to degeneration or modification of their functionality. This study showed that there is an elevated level of isoaspartate in HSA, more HSA aggregates, and increased



levels of free A $\beta$  in the blood of patients with Alzheimer's disease compared to controls. They proposed that deamidation significantly reduces the ability of HSA to bind A $\beta$  and p-tau, suggesting the presence of a bottleneck in the clearance of A $\beta$  and p-tau in Alzheimer's disease, leading to their increased concentration in the brain and facilitating their aggregation<sup>20</sup>. We have observed a 1.3 °C shift in the Albumin peak, and in order to try to correspond it to deamidation we measured pure HSA following a deamidation method. Surprisingly, deamidation increases the melting temperature of HSA, suggesting that the observed shift could originate from such a process. Further proteomic experiments, integrated with thermodynamic analysis are needed to corroborate our observations. However, as evidenced in previous studies of different diseases, the deconvolution of the observed shifts is not a simple task, due to the complexity of the sample and the higher temperatures. Thermal unfolding with associated domains and biomolecule dissociations are reported all together in a DSC scan, this includes the presence of metabolites, lipoproteins and lipid particles playing a role in stabilization or destabilization of the most populated plasma proteins. To address the origin of the observed signatures is a challenge, but unconventional techniques are being developed and we expect that they will shed light into the discovery of novel biomarkers screened by DSC<sup>31</sup>.

v1 Preprint

## Materials and Methods.

**Ethics and Consent.** This observational study followed STROBE guidelines<sup>32</sup>. The protocol CBFIL#22 received the approval from the ethical committee of Fundación Instituto Leloir (Argentina). All participants and/or family members gave their informed consent.

**Volunteer recruitment.** The samples were recruited at Hospital “El Cruce” (Florencio Varela) from Argentina. Cognitive status was determined through the Mini-Mental State Examination (MMSE) with a cutoff of 26/27. The description of the samples is shown in Table 2. The diagnosis of probable AD followed the diagnostic criteria of the National Institute of Neurological and Communicative Disorders and Stroke and the Alzheimer’s disease and Related Disorders Association (NINCDS-ADRDA)<sup>33</sup>.

**Table 2. Descriptive characteristics of the samples across clinical categories**

Clinical categories	Total number of subjects	Sex % Female (Female/Male)	Age (years) Mean (SD)
HE	12	50 (6/6)	71 (8.15)
AD	13	69.2 (9/4)	77 (6.6)

HE, healthy elderly subjects; AD, probable Alzheimer's disease; SD, standard deviation

**Sample Preparation.** Pre-analytical processing and storage of samples was similar between centers. Briefly, a maximum of five mL of whole blood was collected by venipuncture into 6 mL plastic tubes spray-coated with sodium citrate. The tubes were allowed to stand at room temperature (RT) for 30 min, centrifuged at  $1800 \times g$  for 10 min at RT, immediately divided into 250  $\mu$ L aliquots in 0.5 mL polypropylene storage tubes and stored at  $-80^{\circ}\text{C}$  until processing. Before analysis, the samples were defrosted on ice ( $2-8^{\circ}\text{C}$ ) and diluted 1/35 in degassed PBS buffer. The diluted sample was loaded into the DSC sample cell ensuring the absence of trapped air bubbles. Excess sample was removed using a syringe adjusted to the top of the cell. The reference cell was filled with phosphate-buffered saline (PBS).

**Differential Scanning Calorimetry.** The VP-DSC starting temperature was set to  $25^{\circ}\text{C}$  and a final temperature of  $100^{\circ}\text{C}$ , with a scan rate of  $1^{\circ}\text{C}/\text{min}$  and a pre-scan thermostat period of 8 min. The filtering point was set to 8s. The cells were cleaned with concentrated nitric acid (65%) at  $80^{\circ}\text{C}$  for

10 min in the DSC. After cooling, the cells were washed with 500 mL of pure water using an integrated vacuum pump. Hamilton syringes and other equipment were rinsed by a 20% solution of hyperalkaline detergent (DECON 90), pure water, and finally sanitized with 70% ethanol.

**Data Analysis.** Thermograms for all patients were processed using Origin 7 software. The sample thermogram was subtracted from the reference thermogram to obtain the corrected curve. A baseline was established by connecting native and unfolded segments using a cubic polynomial. The thermogram expressed as  $C_p$  in cal/°C vs. temperature was then exported in ASCII format for further processing. The process involves applying a spline fit that interpolates or approximates a smooth curve passing through a set of data points. It starts by multiplying the ASCII file data by 1000 to scale them in kcal, then employing the spline function to tabulate the temperature points from 35 °C to 90 °C at intervals of 0.1 °C. Finally, standardized data were used for the analysis and generation of thermogram profile plots using the ProFit software. The analysis involved five Gaussian functions fitted to the data using the Levenberg-Marquardt algorithm, with a total of 15 parameters corresponding to each peak to the  $T_m$  (transition temperature),  $A_m$  (height), and  $s$  (amplitude) parameters using the ProFit software. Successive fits with one or two Gaussian curves were used to assess the presence of additional signals between peaks 1 and 2.

v1 Preprint

**Acknowledgements.** The authors thank funding from Agencia I+D+i, grants PICT-2020-SERIEA-03739 and PICT-PRH-2019-0017 (to MD) and PICT2019-0656 (to LM) .

v1 Preprint

## References

1. Donovan, J. W., Mapes, C. J., Davis, J. G. & Garibaldi, J. A. A differential scanning calorimetric study of the stability of egg white to heat denaturation. *J. Sci. Food Agric.* **26**, 73–83 (1975).
2. Garbett, N. C., Mekmaysy, C. S., DeLeeuw, L. & Chaires, J. B. Clinical application of plasma thermograms. Utility, practical approaches and considerations. *Methods* **76**, 41–50 (2015).
3. Garbett, N. C., Mekmaysy, C. S., Helm, C. W., Jenson, A. B. & Chaires, J. B. Differential scanning calorimetry of blood plasma for clinical diagnosis and monitoring. *Exp. Mol. Pathol.* **86**, 186–191 (2009).
4. Garbett, N. C., Miller, J. J., Jenson, A. B. & Chaires, J. B. Calorimetry outside the box: a new window into the plasma proteome. *Biophys. J.* **94**, 1377–1383 (2008).
5. Tsvetkov, P. O. *et al.* Differential scanning calorimetry of plasma in glioblastoma: toward a new prognostic / monitoring tool. *Oncotarget* **9**, 9391–9399 (2018).
6. Velazquez-Campoy, A. *et al.* Thermal liquid biopsy for monitoring melanoma patients under surveillance during treatment: A pilot study. *Biochim. Biophys. Acta Gen. Subj.* **1862**, 1701–1710 (2018).
7. Rodrigo, A. *et al.* Thermal Liquid Biopsy (TLB): A Predictive Score Derived from Serum Thermograms as a Clinical Tool for Screening Lung Cancer Patients. *Cancers* **11**, (2019).
8. Vega, S., Garcia-Gonzalez, M. A., Lanas, A., Velazquez-Campoy, A. & Abian, O. Deconvolution analysis for classifying gastric adenocarcinoma patients based on differential scanning calorimetry serum thermograms. *Sci. Rep.* **5**, 7988 (2015).
9. Todinova, S. *et al.* Calorimetry-based profiling of blood plasma from colorectal cancer patients. *Biochim. Biophys. Acta* **1820**, 1879–1885 (2012).
10. Lőrinczy, D. & Ferencz, A. Comparison of deconvoluted plasma DSC curves on patients with solid tumors. *J. Therm. Anal. Calorim.* **142**, 1243–1248 (2020).

11. Todinova, S., Krumova, S., Gartcheva, L., Robeerst, C. & Taneva, S. G. Microcalorimetry of blood serum proteome: a modified interaction network in the multiple myeloma case. *Anal. Chem.* **83**, 7992–7998 (2011).
12. Mehdi, M., Fekecs, T., Zapf, I., Ferencz, A. & Lőrinczy, D. Differential scanning calorimetry (DSC) analysis of human plasma in different psoriasis stages. *J. Therm. Anal. Calorim.* **111**, 1801–1804 (2012).
13. Garbett, N. C., Merchant, M. L., Chaires, J. B. & Klein, J. B. Calorimetric analysis of the plasma proteome: identification of type 1 diabetes patients with early renal function decline. *Biochim. Biophys. Acta* **1830**, 4675–4680 (2013).
14. Lidani, K. C. F. *et al.* Characterization of myocardial injury phenotype by thermal liquid biopsy. *Front Cardiovasc Med* **11**, 1342255 (2024).
15. Michnik, A. *et al.* Differential scanning calorimetry study of blood serum in chronic obstructive pulmonary disease. *J. Therm. Anal. Calorim.* **102**, 57–60 (2009).
16. Danailova, A. *et al.* Thermodynamic Signatures of Blood Plasma Proteome in Neurodegenerative Pathologies. *Int. J. Mol. Sci.* **24**, (2023).
17. Calorimetric monitoring of the serum proteome in schizophrenia patients. *Thermochim. Acta* **572**, 59–64 (2013).
18. Assfaw, A. D., Schindler, S. E. & Morris, J. C. Advances in blood biomarkers for Alzheimer disease (AD): A review. *Kaohsiung J. Med. Sci.* (2024) doi:10.1002/kjm2.12870.
19. Wang, J. *et al.* Deamidation-related blood biomarkers show promise for early diagnostics of neurodegeneration. *Biomark Res* **10**, 91 (2022).
20. Website. <https://doi.org/10.1002/alz.12735> doi:10.1002/alz.12735.
21. Warmack, R. A. *et al.* The l-isoaspartate modification within protein fragments in the aging lens can promote protein aggregation. *J. Biol. Chem.* **294**, 12203–12219 (2019).
22. Sims, J. R. *et al.* Donanemab in Early Symptomatic Alzheimer Disease: The

TRAILBLAZER-ALZ 2 Randomized Clinical Trial. *JAMA* **330**, 512–527 (2023).

23. van Dyck, C. H. *et al.* Lecanemab in Early Alzheimer's Disease. *N. Engl. J. Med.* **388**, 9–21 (2023).
24. Chowdhury, S. & Chowdhury, N. S. Novel anti-amyloid-beta (A $\beta$ ) monoclonal antibody lecanemab for Alzheimer's disease: A systematic review. *Int. J. Immunopathol. Pharmacol.* **37**, 3946320231209839 (2023).
25. Krumova, S. *et al.* Intercriteria analysis of calorimetric data of blood serum proteome. *Biochim. Biophys. Acta Gen. Subj.* **1861**, 409–417 (2017).
26. Todinova, S. *et al.* Red Blood Cells' Thermodynamic Behavior in Neurodegenerative Pathologies and Aging. *Biomolecules* **11**, (2021).
27. Putnam, F. W. *The Plasma Proteins: Structure, Function, and Genetic Control*. (Elsevier, 2012).
28. Krumova, S., Todinova, S. & Taneva, S. G. Calorimetric Markers for Detection and Monitoring of Multiple Myeloma. *Cancers* **14**, (2022).
29. Tsvetkov, P. O. & Devred, F. Plasmatic Signature of Disease by Differential Scanning Calorimetry (DSC). *Methods Mol. Biol.* **1964**, 45–57 (2019).
30. Home. *Alzheimer's Disease and Dementia* <https://alz.org/>.
31. Pepelnjak, M. *et al.* In situ analysis of osmolyte mechanisms of proteome thermal stabilization. *Nat. Chem. Biol.* **20**, 1053–1065 (2024).
32. Vandenbroucke, J. P. *et al.* Strengthening the Reporting of Observational Studies in Epidemiology (STROBE): explanation and elaboration. *Int. J. Surg.* **12**, 1500–1524 (2014).
33. Sperling, R. A. *et al.* Toward defining the preclinical stages of Alzheimer's disease: recommendations from the National Institute on Aging-Alzheimer's Association workgroups on diagnostic guidelines for Alzheimer's disease. *Alzheimers. Dement.* **7**, 280–292 (2011).